

RAPID COMMUNICATION

# Intrinsic phase separation in superconducting $K_{0.8}Fe_{1.6}Se_2$ ( $T_c = 31.8$ K) single crystals

To cite this article: Alessandro Ricci *et al* 2011 *Supercond. Sci. Technol.* **24** 082002

View the [article online](#) for updates and enhancements.

## Related content

- [Intrinsic crystal phase separation in the antiferromagnetic superconductor  \$Rb\_{1-x}Fe\_2Se\_2\$ : a diffraction study](#)  
V Yu Pomjakushin, A Krzton-Maziopa, E V Pomjakushina *et al.*
- [Superconductivity in alkali metal intercalated iron selenides](#)  
A Krzton-Maziopa, V Svitlyk, E Pomjakushina *et al.*
- [Feshbach resonance and mesoscopic phase separation near a quantum critical point in multiband FeAs-based superconductors](#)  
Rocchina Caivano, Michela Fratini, Nicola Poccia *et al.*

## Recent citations

- [Imaging the local electronic and magnetic properties of intrinsically phase separated  \$Rb\_{1-x}Fe\_2Se\_2\$  superconductor using scanning microscopy techniques](#)  
P Dudin *et al*
- [Superconducting selenides intercalated with organic molecules: synthesis, crystal structure, electric and magnetic properties, superconducting properties, and phase separation in iron based-chalcogenides and hybrid organic-inorganic superconductors](#)  
Anna Krzton-Maziopa *et al*
- [Direct observation of microstructures on superconducting single crystals of  \$K\_xFe\_2Se\_2\$](#)   
Masashi Tanaka *et al*



**IOP | ebooks™**

Bringing you innovative digital publishing with leading voices to create your essential collection of books in STEM research.

Start exploring the collection - download the first chapter of every title for free.

## RAPID COMMUNICATION

# Intrinsic phase separation in superconducting $K_{0.8}Fe_{1.6}Se_2$ ( $T_c = 31.8$ K) single crystals

Alessandro Ricci<sup>1</sup>, Nicola Poccia<sup>1</sup>, Bobby Joseph<sup>1</sup>,  
Gianmichele Arrighetti<sup>2</sup>, Luisa Barba<sup>2</sup>, Jasper Plaisier<sup>3</sup>,  
Gaetano Campi<sup>4</sup>, Yoshikazu Mizuguchi<sup>5</sup>, Hiroyuki Takeya<sup>5</sup>,  
Yoshihiko Takano<sup>5</sup>, Naurang Lal Saini<sup>1</sup> and Antonio Bianconi<sup>1</sup>

<sup>1</sup> Department of Physics, Sapienza University of Rome, Piazzale Aldo Moro 2, 00185, Rome, Italy

<sup>2</sup> Institute of Crystallography, National Council of Research, Elettra, 34012, Trieste, Italy

<sup>3</sup> Elettra Synchrotron Center, MCX, 34012, Trieste, Italy

<sup>4</sup> Institute of Crystallography, CNR, via Salaria Km 29.300, Monterotondo Roma, I-00015, Italy

<sup>5</sup> National Institute for Materials Science, 1-2-1 Sengen, Tsukuba, 305-0047, Japan

E-mail: [antonio.bianconi@roma1.infn.it](mailto:antonio.bianconi@roma1.infn.it)

Received 29 April 2011, in final form 19 June 2011

Published 1 July 2011

Online at [stacks.iop.org/SUST/24/082002](http://stacks.iop.org/SUST/24/082002)

## Abstract

Temperature dependent single-crystal x-ray diffraction (XRD) in transmission mode probing the bulk of the newly discovered  $K_{0.8}Fe_{1.6}Se_2$  superconductor ( $T_c = 31.8$  K) using synchrotron radiation is reported. A clear evidence of intrinsic phase separation at 520 K between two competing phases, (i) a first majority magnetic phase with a  $ThCr_2Si_2$ -type tetragonal lattice modulated by the iron  $\sqrt{5} \times \sqrt{5}$  vacancy ordering and (ii) a minority non-magnetic phase having an in-plane compressed lattice volume and a  $\sqrt{2} \times \sqrt{2}$  weak superstructure, is reported. The XRD peaks due to the Fe vacancy  $\sqrt{5} \times \sqrt{5}$  ordering in the majority phase disappear on increasing the temperature to 580 K, well above phase separation temperature, confirming the order–disorder phase transition. The intrinsic phase separation at 520 K between a competing first magnetic phase and a second non-magnetic phase in the normal phase both having lattice superstructures (that imply different Fermi surface topology reconstructions and charge densities) is assigned to a lattice-electronic instability of the  $K_{0.8}Fe_{1.6}Se_2$  system typical of a system tuned at a Lifshitz critical point of an electronic topological transition that gives a multigap superconductor tuned to a shape resonance.

(Some figures in this article are in colour only in the electronic version)

## 1. Introduction

The discovery of iron based superconductors (FeSC) made of FeAs superconducting layers intercalated by different spacer layers [1, 2] has provided a new class of heterostructures at the atomic limit where the lattice structure and its instability are key parameters controlling the complex Fermi surface

topology giving multigap superconductivity stable at high temperature. Recently a new system  $A_xFe_{2-y}Se_2$ , made of FeSe superconducting layers intercalated by spacer layers  $A = K$  [3, 4], Cs [5, 6], Rb [7], (Tl, Rb) [8], (Tl, K) [9], etc, has provided an additional system with a different Fermi surface topology. The most striking common feature of the FeSC is the presence of an active layer of FePn or FeCh (Pn:

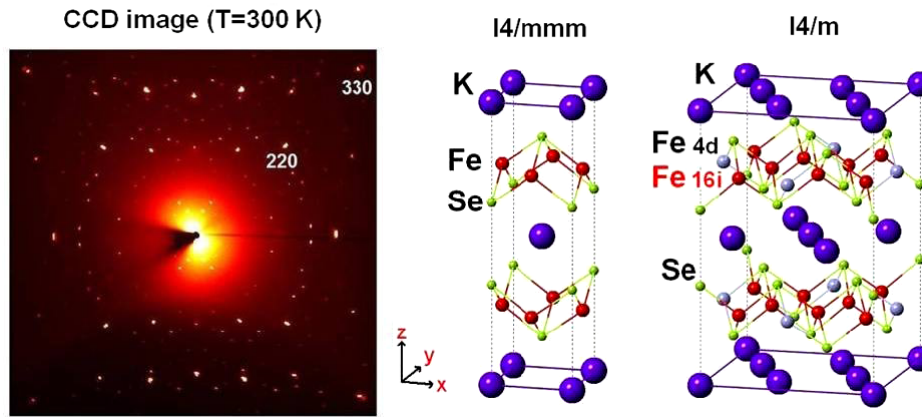


**Figure 1.** Single-crystal x-ray diffraction pattern (CCD image) of  $\text{K}_{0.8}\text{Fe}_{1.6}\text{Se}_2$  at 300 K. Structural models of the basic ( $I4/mmm$ ) and larger ( $I4/m$ ) unit-cells of the 122-type tetragonal structure are also shown.

pnictogen and Ch: chalcogen) edge sharing tetrahedrons. The  $\text{A}_x\text{Fe}_{2-y}\text{Se}_2$  show multigap superconductivity with concentric multiple Fermi surfaces as has been proposed in the shape resonance scenario for multigap superconductors made of heterostructures at the atomic limit [10]. Heterostructures of metallic layers at the atomic limit provide metals with mini bands where high  $T_c$  is controlled by the fine tuning of the chemical potential in the range of tens to hundreds of meV around Lifshitz electronic topological transitions [10]. At such a low energy scale the fine tuning of the lattice structure of the superconducting active layers in these heterostructures at the atomic limit is of high importance. The structure of the active superconducting layers is controlled by changing the spacer layers via the misfit strain between the active layers and the spacer layers as in cuprates [11]. The average crystal structure of  $\text{A}_x\text{Fe}_{2-y}\text{Se}_2$  at room temperature has already been established by different structural studies [12–19]. These studies revealed the structure of  $\text{A}_x\text{Fe}_{2-y}\text{Se}_2$  to be of ‘122’ type, with the presence of a Fe-square lattice decorated by a regular array of vacancies [12–19] and hence a unit-cell structure five times larger than the basic  $\text{ThCr}_2\text{Si}_2$ -type tetragonal unit-cell. Figure 1(b) shows a schematic view of the basic ‘122’ type unit-cell and an expanded cell which can accommodate ordered vacancies at one of the Fe-sites. Temperature dependent neutron diffraction studies have revealed that the structural and magnetic phase transitions are related with the vacancy ordering in this system [13, 14, 18].

Here we present a temperature dependent single-crystal x-ray diffraction study of the  $\text{K}_{0.8}\text{Fe}_{1.6}\text{Se}_2$  superconductor ( $T_c = 31.8$  K) to understand the structural dynamics of the system. We use high energy x-ray synchrotron radiation diffraction in transmission mode which allows us to probe the intrinsic bulk structure. We confirm previous works showing that the system undergoes an order–disorder transition at 580 K, as evidenced by the disappearance of the superstructure peaks due to the vacancy ordering. The superstructure peak intensities follow the same behavior upon heating and cooling with no detectable temperature hysteresis.

The main discovery of this work is that, unlike the earlier diffraction studies using powder samples [13, 14], our

high-resolution single-crystal x-ray diffraction data show the occurrence of a phase separation in  $\text{K}_{0.8}\text{Fe}_{1.6}\text{Se}_2$  below 520 K (about 60 K lower than the vacancy ordering temperature) between a first in-plane expanded majority phase and a second in-plane compressed minority phase. Moreover, on decreasing the temperature below 520 K a new set of superstructure diffraction peaks associated with the appearance of the minority phase is observed. These results constitute clear evidence of an intrinsic phase separation in the 122 chalcogenides  $\text{K}_{0.8}\text{Fe}_{1.6}\text{Se}_2$ , which is assigned to the lattice instability of an electronic system near a Lifshitz critical point where a majority magnetic phase competes with the superconducting multigap phase where  $T_c$  is amplified by a shape resonance [10]. The competition between the two phases provides a complex phase separation where the two lattice structures show different lattice reconstructions.

## 2. Experimental details

Single crystals of nominal composition  $\text{K}_{0.8}\text{Fe}_{1.6}\text{Se}_2$  were prepared following the method described in [4]. The actual composition of the crystal was estimated to be  $\text{K}:\text{Fe}:\text{Se} = 0.6:1.5:2$  using an average of four points of the EDX measurements. The resistivity and magnetization studies showed the presence of a sharp superconducting transition at about 31.8 K ( $T_c$  onset 33 K) [4]. The x-ray diffraction (XRD) data on the single-crystal samples were obtained at the XRD1 beamline of the ELETTRA synchrotron radiation facility in Trieste. The samples were oriented by means of a K diffractometer with a motorized goniometric  $X$ – $Y$  stage head and a Mar-Research 165 mm CCD camera. The data were collected in transmission mode, with a photon energy of  $\sim 20$  keV ( $\lambda = 0.61992$  Å), selected from the source by a double-crystal Si(111) monochromator. The x-ray diffracted beams were detected by a 2D CCD detector (MAR-Research), kept at a distance of around 70 mm from the sample. Data from a  $\text{LaB}_6$  standard were also collected for calibration. Measurements were conducted between 80 and 600 K with a temperature step of 3 K for the heating (80–600 K) and 2 K for the cooling (600–80 K) runs. For the measurements in

the range of 80–300 K, the sample temperature was varied and controlled by means of a cryocooler (700 series Oxford Cryosystems). For the measurements in the temperature range 300–600 K, a heat blower facility (Oxford Danfysik gas blower, DGB-0002) was used. In both cases, the temperature control was better than  $\pm 1$  K. The single-crystal x-ray diffraction images measured were properly processed using the FIT2D program. The processed images were analyzed using a matlab<sup>®</sup> based software package developed in-house.

### 3. Results

A typical single-crystal XRD as-obtained pattern at 300 K is shown in figure 1. The pattern at room temperature is similar to the one reported in [15] for a similar compound. The crystal displays a tetragonal  $\text{ThCr}_2\text{Si}_2$ -type diffraction pattern with overlapping superstructure peaks. Structural models corresponding to the basic and extended unit-cells are also shown in figure 1. The extended unit-cell has two sites for the Fe (4d and 16i), which permits the vacancies to preferentially occupy one of the sites and order. The vacancy ordering observed at room temperature gives rise to the superstructure diffracted spots that can be indexed with a  $\sqrt{5} \times \sqrt{5} \times 1$  expanded unit-cell (symmetry  $I4/m$ ) of the basic  $\text{ThCr}_2\text{Si}_2$  structure [13–19]. The  $a, b$  lattice parameters corresponding to the basic unit-cell are determined from the pattern shown in figure 1. The obtained value is  $a = b \approx 4.01(3)$  Å. A careful observation of the image shown in figure 1 reveals that the principal diffraction spots are surrounded by superstructure peaks forming a group of eight reflections (see inset in figure 2 lower panel) in agreement with the data reported for similar systems at room temperature [15, 18].

Diffraction patterns with superstructure peaks around the beam center, at five selected temperatures, are shown in the upper panel of figure 2. At 600 K, except for the principal diffraction spots, there are no other superstructure features. The data collected at 525 K show a single group of bright spots in figure 1(a) that can be clearly identified as belonging to the group of eight superstructure reflections around each principal XRD spot (see e.g. the inset in figure 2) identified as the  $(1/5, 3/5, 0)$  diffraction spots in the reciprocal space. The occurrence of eight well defined superstructure spots can be understood as the twin structure described in [18], as described for the  $\text{TlFe}_{2-x}\text{Se}_2$  system by Häggström *et al* [20]. The peak intensity variation for one of the superstructure peaks of the first type during the heating run from 80 to 600 K is shown in the lower panel of figure 2. On increasing the temperature, the intensity of these superstructures starts to slowly decrease at around 520 K and finally disappears at around 580 K.

In addition to the first known set of superstructure peaks, we observe the appearance of a second new set of superstructure peaks below 520 K (see figure 2, upper panel, frame marked as 510 K), assigned to the  $\sqrt{2} \times \sqrt{2}$  superstructure.

Figure 3 shows the temperature evolution of the (220) principal diffraction spot. Below 520 K, the peak splits into two components with asymmetric intensities that become more evident in the low temperature range. The complete evolution

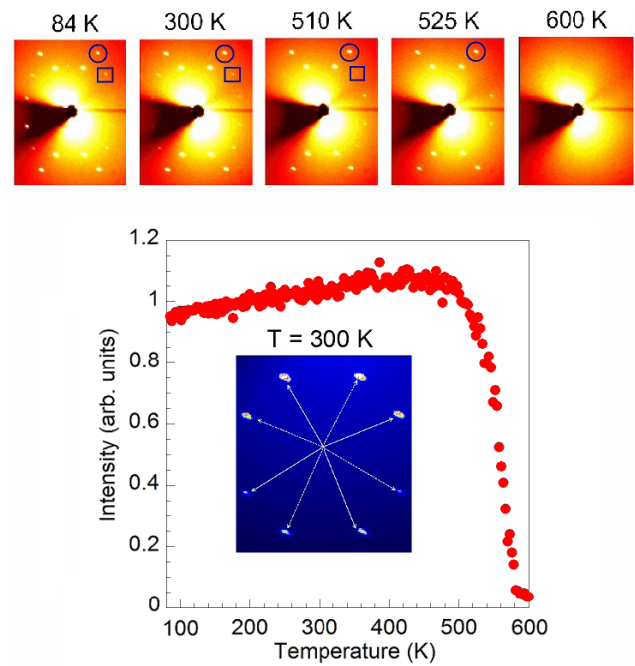


**Figure 2.** (Upper panel) temperature evolution of the spots due to superstructures around the beam center at five selected temperatures. The first set of superlattice peaks ( $\sqrt{5} \times \sqrt{5}$ ) are marked with open circles and the second set of weak superstructure peaks ( $\sqrt{2} \times \sqrt{2}$ ) are marked by squares. Starting from high temperature, at 600 K there are no superstructure spots, at 525 K only the first set of superstructure is detected, and in the frames recorded at 510 K and lower temperatures both superstructures are detected. (Lower panel) the intensity of the superstructure peaks (of the first  $\sqrt{5} \times \sqrt{5}$  type, marked with circles in the upper panel) during a heating run from 80 to 600 K. The inset shows the superstructure peaks (of the first  $\sqrt{5} \times \sqrt{5}$  type, marked with circles in the upper panel) as a group of eight spots around the (100) peak position.

of the (220) peak between 300 and 600 K during the heating run, reconstructed from the CCD image analysis, is shown in the middle panel as a 3D plot of intensity versus temperature and reciprocal lattice wavevector. A clear peak splitting is evident below 520 K. The relative intensities of the diffraction spots of the two crystal lattices permit us to make a rough estimate of the percentage of the two phases. The bottom panel of figure 3 shows the change in the normalized intensities of the majority in-plane expanded phase and the minority in-plane compressed phase. The majority phase has a weight of about 79% at 350 K which becomes 100% above 525 K, with a corresponding vanishing of the intensity of the reflections due to the in-plane compressed minority phase. These data show clearly the intrinsic phase separation in the  $\text{K}_{0.8}\text{Fe}_{1.6}\text{Se}_2$  superconductor below 520 K.

In figure 4, we summarize the results of the present study. During cooling from the disordered single phase at 600 K, the superstructure peaks due to  $\sqrt{5} \times \sqrt{5}$  vacancy ordering start to appear at around 580 K, at the same temperature as these peaks disappear in the heating run. In other words, the temperature dependence of the peak intensity variation seems to be identical in the heating and cooling runs.

In contrast, the peak intensity of the (220) satellite during the heating and cooling shows a sharp intensity drop at

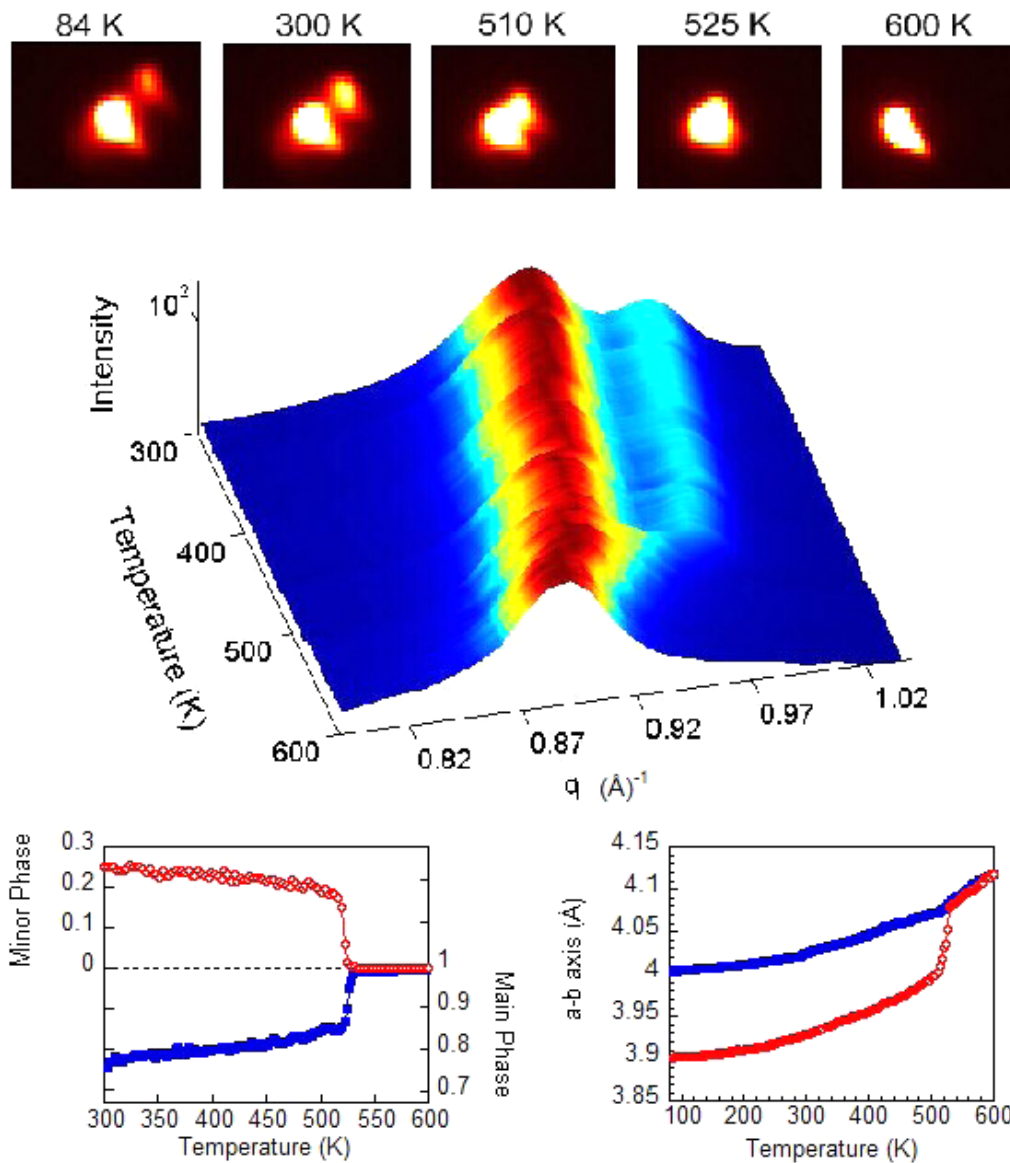


**Figure 3.** (Upper panel) temperature evolution of the (220) peaks at five selected temperatures. (Middle panel) a three-dimensional intensity plot of the (220) peak as a function of temperature for the heating run from 300 to 600 K. Below 520 K, the (220) peaks split, indicating the appearance of a second in-plane compressed minority phase. (Lower left panel) the normalized peak intensities of the first main phase and the second minority phase. (Lower right panel) the in-plane lattice parameter variation with temperature showing the phase separation at 520 K.

about 520 K, with a temperature hysteresis of about 10 K. This implies that the intrinsic phase separation occurring at this temperature is primarily of first order nature, unlike the continuous second order nature of the superstructure peak transition at 580 K. Importantly, the superstructure peak intensity shows no particular change at the phase separation temperature of 520 K. However, as shown in figure 2, a new set of  $\sqrt{2} \times \sqrt{2}$  superstructure peaks starts to appear at 520 K. The temperature dependence of the integrated intensities of these new superstructure peaks in a limited temperature range during a cooling run is shown in the inset of the left panel in figure 4. The principal diffraction spots of the minority in-plane compressed phase and the new set of  $\sqrt{2} \times \sqrt{2}$  superstructure peaks appear at the same temperature, indicating an intimate connection between the two. Further work is

ongoing to characterize this superstructure and it will be the subject of a longer paper.

#### 4. Discussion

We first discuss the ordering of iron vacancies in the majority in-plane expanded phase. The first thing to notice is that the temperature evolution of the associated  $\sqrt{5} \times \sqrt{5}$  superstructure spots is in agreement with previous neutron diffraction studies [13, 14] on similar systems. The Néel temperature estimated from the neutron diffraction studies is around 560 K, below the order-disorder transition observed at 590 K [13, 14], thus presenting a close analogy between the structural and magnetic transitions observed in the '1111' family of FeSCs [1, 2, 21, 22] and the new

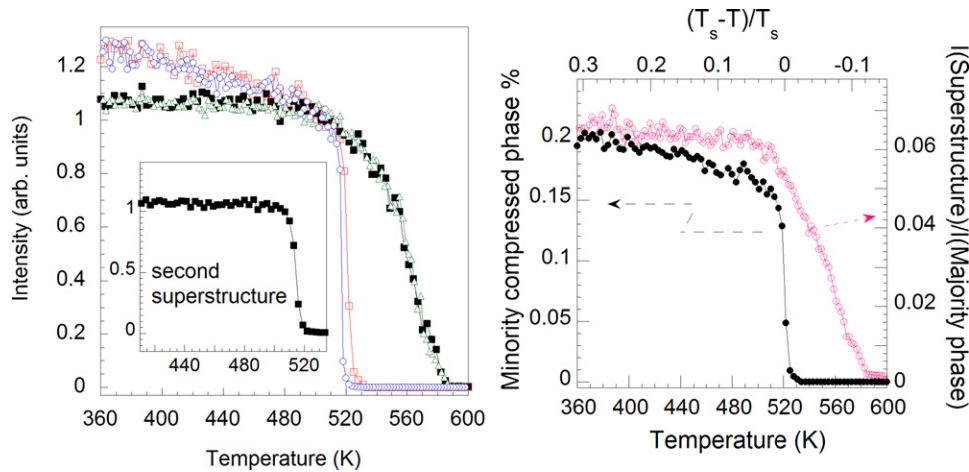


**Figure 4.** (Left panel) the continuous temperature evolution of the  $\sqrt{5} \times \sqrt{5}$  superstructure satellite intensity during the heating (open triangles) and cooling (filled squares) runs. The sharp temperature drop of the minority phase during the heating (open squares) and its appearance on cooling (open circles) runs can be seen. The inset in the left panel shows the temperature dependence of the integrated intensities of the second weak set of  $\sqrt{2} \times \sqrt{2}$  superstructure peaks (filled squares) (refer to the spots in the open squares in figure 2). During the cooling run the  $\sqrt{2} \times \sqrt{2}$  superstructure peaks show the same temperature onset as the principal XRD diffraction spots of the minority in-plane compressed phase. (Right panel) the variation of the probability of the minority in-plane compressed phase around the phase separation temperature (520 K) (filled dots) and the temperature variation of the ratio (open circles) between the intensity of the  $\sqrt{5} \times \sqrt{5}$  iron vacancy superstructure satellites and the principal diffraction spots of the in-plane expanded majority phase.

$A_x\text{Fe}_{2-y}\text{Se}_2$  systems. Interestingly, the magnetic and structural transitions are concurrent in the structurally identical ‘122’ pnictides [1, 2, 23]. As already discussed, the temperature dependence of the appearance and disappearance of the  $\sqrt{5} \times \sqrt{5}$  superstructure is continuous, without a significant temperature hysteresis, indicating the transition to be of second order.

Let us now discuss the new intrinsic phase separation observed here. Earlier structural studies using powder samples [13, 14] have not revealed such a transition in  $\text{K}_{0.8}\text{Fe}_{1.6}\text{Se}_2$  superconductors. Indeed single-crystal studies provide more insights into the phase separation properties, as revealed in the case of ‘1111’ FeSCs [1, 2, 21, 22]. It is to be stressed that there is the simultaneous sharp appearance of a new set of superstructure peaks together with the minority in-plane compressed phase by decreasing the temperature to below 520 K.

A recent  $^{57}\text{Fe}$  Mössbauer study on the  $\text{K}_x\text{Fe}_{2-y}\text{Se}_2$  system revealed abrupt changes in the magnetic fraction of the sample at about a similar temperature [24] to the phase separation observed here. An earlier Mössbauer study [20] on  $\text{TlFe}_{2-y}\text{Se}_2$  showed that at lower temperature the anti-ferromagnetic (AFM) and paramagnetic fractions coexist with the majority phase to be of AFM nature. The temperature evolution of the magnetic fraction observed in the Mössbauer studies of  $\text{K}_x\text{Fe}_{2-y}\text{Se}_2$  is also of similar nature. These results indicate the existence of two coexisting phases in the low temperature region of  $\text{K}_x\text{Fe}_{2-y}\text{Se}_2$ . Very recent differential scanning calorimetric measurements on superconducting  $\text{Cs}_x\text{Fe}_{2-y}\text{Se}_2$  show two distinct heat-flow peaks, a larger one at higher temperature and a weaker one at lower temperature [18], further supporting two possible phases in superconducting  $\text{K}_x\text{Fe}_{2-y}\text{Se}_2$ .

The present observation of the intrinsic phase separation in  $\text{K}_x\text{Fe}_{2-y}\text{Se}_2$  indicates the importance of the lattice complexity of the  $A_x\text{Fe}_{2-y}\text{Se}_2$  systems. Indeed the phase diagram involving Fe–Se shows the possibility of coexisting phases for different ratios between Fe and Se [25], consistent with the extreme sensitivity of the chemical composition to the superconducting properties of FeSe [26]. The coexisting chalcogen heights observed in the doped ternary chalcogenides [27] are found to be more pronounced in the  $A_x\text{Fe}_{2-y}\text{Se}_2$  systems [16–18]. The  $\text{K}_x\text{Fe}_{2-y}\text{Se}_2$  system with its interesting temperature dependent vacancy ordering and competing mesoscopic phases recalls the oxygen ordering effects on the superconductivity of cuprates [28, 37]. This intrinsic phase separation is assigned to a generic feature of multigap high temperature superconductors where the system is on the verge of phase separation like in FeAs superlattices [29] and cuprates [30–37]. The data show a clear case of the competition between two electron fluids producing a mesoscopic frustrated phase separation between a majority magnetic metallic phase with  $\sqrt{5} \times \sqrt{5}$  ordered defects and a superconducting phase with a second  $\sqrt{2} \times \sqrt{2}$  superstructure order with different charge densities; i.e. two striped metallic systems with two different lattice superstructures that will induce a different Fermi surface reconstruction with mini bands and pseudogaps of a few tens of meV. The present scenario for  $A_x\text{Fe}_{2-y}\text{Se}_2$  is similar to the case of overdoped cuprates where two phases compete with different dopings [35–38].

## 5. Conclusions

We have reported temperature dependent single-crystal x-ray diffraction studies of the newly discovered  $\text{K}_{0.8}\text{Fe}_{1.6}\text{Se}_2$

superconductor using synchrotron radiation in transmission mode. The basic structure of the sample at room temperature is found to be tetragonal  $\text{ThCr}_2\text{Si}_2$ -type, modulated by vacancy ordering induced superstructures together with a coexisting minority phase with associated different superstructures. The phase separation appears at 520 K, above which the minority in-plane compressed phase merges with the majority in-plane expanded phase. There is a temperature hysteresis of about 10 K, indicating the phase separation transition to be first order. The superstructure peaks corresponding to the main Fe vacancy ordering disappear at 580 K, without noticeable temperature hysteresis, confirming the order–disorder second order phase transition at high temperatures above the phase separation temperature. The present scenario shows that a heterostructure at the atomic limit made of a superlattice of metallic layers [39, 40] like iron based superconductors tuned at a Lifshitz critical point [10], is on the verge of a lattice catastrophe for phase separation between the two types of metals. In the phase separation regime a fine tuning of their Fermiology via two lattice superstructures provides a first itinerant magnetic phase with low lattice symmetry and a second high temperature superconductor tuned at a shape resonance [10] in a landscape of complex phase separation that was called the ‘superstripes’ scenario in cuprates [36].

## References

- [1] Johnston D C 2010 The puzzle of high temperature superconductivity in layered iron pnictides and chalcogenides *Adv. Phys.* **59** 803–1061
- [2] Paglione J and Greene R L 2010 High-temperature superconductivity in iron-based materials *Nature Phys.* **6** 645–58
- [3] Guo J *et al* 2010 Superconductivity in the iron selenide  $\text{K}_x\text{Fe}_2\text{Se}_2$  ( $0 < x < 1.0$ ) *Phys. Rev. B* **82** 180520
- [4] Mizuguchi Y *et al* 2010 Transport properties of the new Fe-based superconductor  $\text{K}_x\text{Fe}_2\text{Se}_2$  ( $T_c = 33$  K) arXiv:1012.4950
- [5] Krzton-Maziopa A *et al* 2011 Synthesis and crystal growth of  $\text{Cs}_{0.8}(\text{FeSe}_{0.98})_2$ : a new iron-based superconductor with  $T_c = 27$  K *J. Phys.: Condens. Matter* **23** 052203
- [6] Shermadini Z *et al* 2011 Coexistence of magnetism and superconductivity in the iron-based compound  $\text{Cs}_{0.8}(\text{FeSe}_{0.98})_2$  arXiv:1101.1873
- [7] Wang A F *et al* 2011 Superconductivity at 32 K in single-crystalline  $\text{Rb}_x\text{Fe}_{2-y}\text{Se}_2$  *Phys. Rev. B* **83** 060512
- [8] Wang H-D *et al* 2011 Superconductivity at 32 K and anisotropy in  $\text{T}_{10.58}\text{Rb}_{0.42}\text{Fe}_{1.72}\text{Se}_2$  crystals *Europhys. Lett.* **93** 47004
- [9] Fang M *et al* 2010 Fe-based high temperature superconductivity with  $T_c = 31$  K bordering an insulating antiferromagnet in  $(\text{Tl}, \text{K})\text{Fe}_x\text{Se}_2$  crystals arXiv:1012.5236
- [10] Innocenti D *et al* 2011 Shape resonance for the anisotropic superconducting gaps near a Lifshitz transition: the effect of electron hopping between layers *Supercond. Sci. Technol.* **24** 015012
- Innocenti D *et al* 2010 Resonant and crossover phenomena in a multiband superconductor: tuning the chemical potential near a band edge *Phys. Rev. B* **82** 184528
- [11] Bianconi A, Agrestini S, Bianconi G, Castro D and Saini N 2000 Lattice-charge stripes in the high- $T_c$  superconductors *Stripes and Related Phenomena* vol 8 *Selected Topics in Superconductivity* ed A Bianconi and N L Saini (Boston, MA: Springer) chapter 2, pp 9–25 [http://dx.doi.org/10.1007/0-306-47100-0\\_2](http://dx.doi.org/10.1007/0-306-47100-0_2)
- [12] Wang Z *et al* 2011 Microstructure and ordering of iron vacancies in the superconductor system  $\text{K}_y\text{Fe}_x\text{Se}_2$  as seen via transmission electron microscopy *Phys. Rev. B* **83** 140505
- [13] Bao W *et al* 2011 A novel large moment antiferromagnetic order in  $\text{K}_{0.8}\text{Fe}_{1.6}\text{Se}_2$  superconductor arXiv:1102.0830
- [14] Bao W *et al* 2011 Vacancy tuned magnetic high- $T_c$  superconductor  $\text{K}_x\text{Fe}_{2-x/2}\text{Se}_2$  arXiv:1102.3674
- [15] Zavalij P *et al* 2011 On the structure of vacancy ordered superconducting potassium iron selenide arXiv:1101.4882
- [16] Bacsá J *et al* 2011 Cation vacancy order in the  $\text{K}_{0.8+x}\text{Fe}_{1.6-y}\text{Se}_2$  system: five-fold cell expansion accommodates 20% tetrahedral vacancies *Chem. Sci.* **2** 1054
- [17] Wang D M, He J B, Xia T L and Chen G F 2011 Effect of varying iron content on the transport properties of the potassium-intercalated iron selenide  $\text{K}_x\text{Fe}_{2-y}\text{Se}_2$  *Phys. Rev. B* **83** 132502
- [18] Pomjakushin V Yu *et al* 2011 Iron-vacancy superstructure and possible room-temperature antiferromagnetic order in superconducting  $\text{Cs}_y\text{Fe}_{2-x}\text{Se}_2$  *Phys. Rev. B* **83** 144410
- [19] Ye F *et al* 2011 Common structural and magnetic framework in the  $\text{A}_2\text{Fe}_4\text{Se}_5$  superconductors arXiv:1102.2882
- [20] Häggström L 1991 A Mössbauer study of antiferromagnetic ordering in iron deficient  $\text{TlFe}_{2-x}\text{Se}_2$  *J. Magn. Magn. Mater.* **98** 37–46
- [21] Ricci A, Fratini M and Bianconi A 2009 The tetragonal to orthorhombic structural phase transition in multiband FeAs-based superconductors *J. Supercond. Novel Magn.* **22** 305–8
- [22] Ricci A *et al* 2010 Structural phase transition and superlattice misfit strain of  $\text{RFeAsO}$  ( $\text{R} = \text{La}, \text{Pr}, \text{Nd}, \text{Sm}$ ) *Phys. Rev. B* **82** 144507
- Jesche A, Krellner C, de Souza M, Lang M and Geibel C 2010 Coupling between the structural and magnetic transition in  $\text{CeFeAsO}$  *Phys. Rev. B* **81** 134525
- Tian W *et al* 2010 Interplay of Fe and Nd magnetism in  $\text{NdFeAsO}$  single crystals *Phys. Rev. B* **82** 060514
- [23] Rotter M *et al* 2008 Spin-density-wave anomaly at  $140\text{K}$  in the ternary iron arsenide  $\text{BaFe}_2\text{As}_2$  *Phys. Rev. B* **78** 020503
- [24] Ryan D H *et al* 2011  $^{57}\text{Fe}$  Mössbauer study of magnetic ordering in superconducting  $\text{K}_{0.80}\text{Fe}_{1.76}\text{Se}_2$  single crystals *Phys. Rev. B* **83** 104526
- [25] Predel B 1995 *Fe–Se (Iron–Selenium) (Materials—The Landolt–Börnstein Database)* ed O Madelung (Berlin: Springer) <http://www.springermaterials.com/index/bookdoi/10.1007/b55397>
- [26] McQueen T M *et al* 2009 Extreme sensitivity of superconductivity to stoichiometry in  $\text{Fe}_{1+x}\text{Se}$  *Phys. Rev. B* **79** 014522
- [27] Joseph B *et al* 2010 Evidence of local structural inhomogeneity in  $\text{FeSe}_{1-x}\text{Te}_x$  from extended x-ray absorption fine structure *Phys. Rev. B* **82** 020502
- [28] Fratini M *et al* 2010 Scale-free structural organization of oxygen interstitials in  $\text{La}_2\text{CuO}_{4+y}$  *Nature* **466** 841
- [29] Caivano R *et al* 2009 Feshbach resonance and mesoscopic phase separation near a quantum critical point in multiband FeAs-based superconductors *Supercond. Sci. Technol.* **22** 014004
- [30] Gorkov L and Teitelbaum G 2005 Pseudogap regime in high- $T_c$  cuprates as a manifestation of a frustrated phase separation (NMR view) *Physica B* **359–361** 509–11
- [31] Dagotto E 2005 Complexity in strongly correlated electronic systems *Science* **309** 257–62
- [32] de Mello E V L and Dias D H N 2007 Phase separation and the phase diagram of cuprate superconductors *J. Phys.: Condens. Matter* **19** 086218

- [33] Bishop A R 2008 HTC oxides: a collusion of spin, charge and lattice *J. Phys.: Conf. Ser.* **108** 012027
- [34] Müller K A 2007 On the superconductivity in hole doped cuprates *J. Phys.: Condens. Matter* **19** 251002
- [35] Innocenti D *et al* 2009 A model for liquid-stripped liquid phase separation in liquids of anisotropic polarons *J. Supercond. Novel Magn.* **22** 529
- [36] Bianconi A 2000 Superstripes *Int. J. Mod. Phys. B* **14** 3289–97
- [37] Poccia N, Ricci A and Bianconi A 2011 Fractal structure favoring superconductivity at high temperatures in a stack of membranes near a strain quantum critical point *J. Supercond. Novel Magn.* **24** 1195–200
- [38] Kugel K I, Rakhmanov A L, Sboychakov A O, Poccia N and Bianconi A 2008 Model for phase separation controlled by doping and the internal chemical pressure in different cuprate superconductors *Phys. Rev. B* **78** 165124
- [39] Bianconi A 1994 On the possibility of new high  $T_c$  superconductors by producing metal heterostructures as in the cuprate perovskites *Solid State Commun.* **89** 933–6
- [40] Ricci A *et al* 2010 On the possibility of a new multiband heterostructure at the atomic limit made of alternate  $\text{CuO}_2$  and FeAs superconducting layers *Supercond. Sci. Technol.* **23** 052003